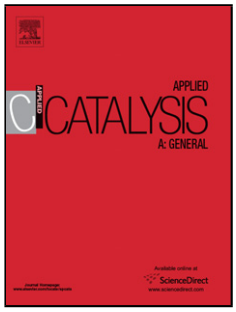

Title: Heteropoly acid supported on silicalite−1 possesing intracrystalline nanovoids prepared using biomass − an efficient and recyclable catalyst for esterification of levulinic acid

Authors: K. Manikandan, K.K. Cheralathan

PII: S0926-860X(17)30435-0
DOI: http://dx.doi.org/10.1016/j.apcata.2017.09.007
Reference: APCATA 16401

To appear in: *Applied Catalysis A: General*

Received date: 30-6-2017
Revised date: 23-8-2017
Accepted date: 4-9-2017

Please cite this article as: K.Manikandan, K.K.Cheralathan, Heteropoly acid supported on silicalite−1 possesing intracrystalline nanovoids prepared using biomass − an efficient and recyclable catalyst for esterification of levulinic acid, Applied Catalysis A, Generalhttp://dx.doi.org/10.1016/j.apcata.2017.09.007

Heteropoly acid supported on silicalite-1 possesing intracrystalline nanovoids prepared using biomass - an efficient and recyclable catalyst for esterification of levulinic acid

K. Manikandan and K. K. Cheralathan*

Department of Chemistry, School of Advanced Sciences, VIT University, Vellore, 632014, India

*Corresponding author e-mail: cheralathan.k@vit.ac.in

Graphical abstract

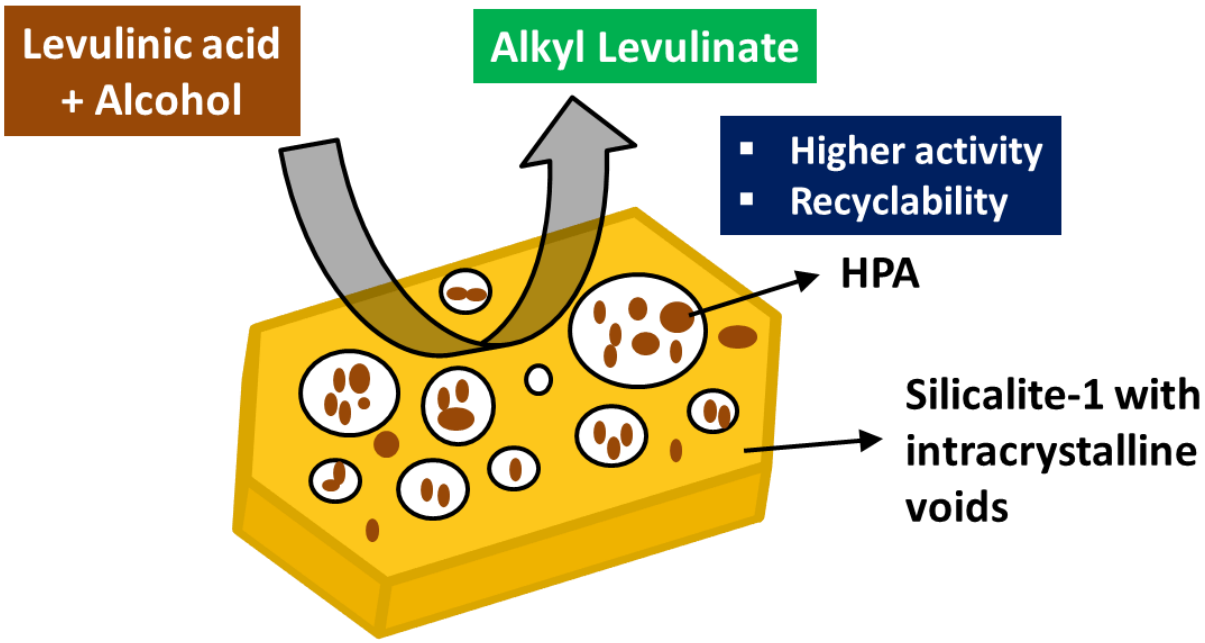

Highlights

- Silicalite-1 with intracrystalline nanovoids was prepared using corn stem pith powder
- The prepared silicalite-1 possessed larger external surface area and led to higher dispersion of heteropoly acid
- ^{31}P-MAS NMR and XPS results indicated interfacial bond formation between support and heteropoly acid
- The supported catalyst showed better catalytic activity in esterification of levulinic acid
- The catalyst was stable even after four recycles and no leaching of heteropoly acid observed

Silicalite-1, a silicious zeolite having intracrystalline nanovoids in addtion to its intrinsic micropores was prepared under hydrothermal condition using corn stem pith powder as a hard template. The zeolite was used as a support for 12-phosphotungstic acid (HPA) and the resulted catalyst was characterized using powder X-ray diffraction, N_2 adsorption, scanning electron microscopy, transmission electron microscopy, Fourier transform infrared spectroscopy, ^{31}P - magic angle spinning nuclear magnetic resonance spectroscopy (^{31}P-MAS NMR), X-ray photoelelctron spectroscopy, ultraviolet-visible spectroscopy and temperature programmed desorption of ammonia. Supporting HPA on the zeolite containing nanovoids improved dispersion of HPA and hence increased the number of accessible acid sites. X-ray photoelectron and ^{31}P-MAS NMR spectra indicated interfacial bond formation between the zeolite surface and HPA. The supported HPA was tested as a hetergeneous catalyst for esterifiation of levulinic acid with 1-propanol, 1-butanol and 1-heptanol. Heteropoly acid supported on the zeolite with intracrytalline nanovoids exhibited enhanced catalytic activity and the activity was stable even after four recycles.

Key words: Zeolite; heteropoly acid; levulinic acid; esterification; biofuel

Introduction

Amongst Keggin series of heteropoly acids, $H_3PW_{12}O_{40}$ (12-phosphotungstic acid (HPA)) has been widely used as a catalyst because of its high proton conductivity, stable nature and strong Bronsted acidity [1]. However, industrial use of HPA is limited, because of its solubility in polar solvents and small surface area [2,3]. Hence, when used in heterogeneous catalysis, there is a need to support HPA on suitable solid, which will improve dispersion, acidity and stability. In the last few decades, supported HPA catalyst has been widely studied for synthetically important transformations of organic molecules [4-13]. Carbon [14-16] porous silica [17-20] and zeolites [4,21,22] are some of the preferred materials for supporting HPA. Mesoporous silicas are better supports for heteropoly acids since they possess higher surface areas, larger pore sizes and weak acidity. However, in general, due to their amorphous nature, mesoporous silicas are not stable under hydrothermal conditions [23]. In this aspect, zeolites are suitable candidates as supports for HPA since they are crystalline and hydrothermally more stable at the same time possess large surface area. But zeolites are microporous, so at higher loadings of heteropoly acids, pore blocking and resulted decrease in surface area are observed [21,22]. A recent report indicates that mesoporous and hierarchical zeolites can be better candidates for supporting HPA as they have pores larger than micropores in them which allow higher loadings of HPA and better catalytic activity [4,21,22].

Mesoporous and hierarchical zeolites having pores larger than micropores could be prepared by various approaches [24–26]. Surfactants [27], carbon templates [28], polymers [29] and preformed scaffolds [30,31] are some of the templates used for the preparation of hierarchically porous zeolite. The non-templated approaches such as desilication and dealumination are also known [32-34].Natural materials have also been utilized for the preparation of hierarchically porous zeolites. Vidal and co-workers have shown that using the plant, Equisetum arvense as template, beta zeolite with hierarchical porosity could be prepared [35]. Valtchev et al. used eggshell membrane and performed secondary growth of zeolite crystals on the membrane to get hierarchical MFI zeolite [36]. Cao et al. followed similar seeded growth strategy to get hierarchical silicalite-1 using cedar wood and bamboo as templates [37-39] .Cui Li et al. reported preparation of hierarchically structured siliclite-1 monoliths using resorcinol-formaldehyde aerogel as the template [40]. ZSM-5 monolith with hierarchical pores using

polyurethane as scaffold has been reported recently by Zhao and co-workers [41]. From our group, we have recently shown preparation of hierarchically porous MFI monoliths by steam assisted conversion using corn and sorghum stem piths as hard templates [42]. The resulted monoliths possessed macropores and mesopores in addition to micropores and exhibited better catalytic activity than conventional ZSM-5 zeolite [42]. Corn and sorghum stem pith are agricultural wastes so they are cheap and their production is sustainable. Hence this method offered a cost effective and sustainable way to prepare hierarchical MFI zeolite monoliths.

In the recent years, upgradation of biomass for the production of fuels and chemcial feed stocks is gaining importance [43,44]. Levulinic acid (LA) is one of the important platform chemicals obtained by degradation of biomass [45]. Hydrogenation of levulinic acid into γ-valarolactone has been reported by many researchers as a way for valarization of LA [46-48]. Esterfication of LA is an another method to convert levulinic acid into valuable products and levulinic acid esters are known to be fuel additives and fragrance and flavouring agents [49]. Different materials were studied as heterogeneous catalysts for esterfication of levulinic acid. Heteropoly acid supported on different materials have been studied as acid catalysts for esterification of LA with different alcohols [22,44,50]. Esterfication of LA with benzyl alcohol over sulphated grapheen oxide monolith has been reported by Akhil and Yadav [51]. 20 wt% dodecotungstophosphoric acid supported on clay was found to be an efficient catalyst to obtain butyl levulinate from LA and n-butyl alcohol [50]. Tajero et al. found that gel-type ion exchange resins were suitable candidates for preparation of butyl levulinate at lower temperatures than zeolites and montmorillonite supported HPA [52]. Kalpana et al studied H-Beta, H-MOR, HY and H-ZSM-5 zeolites for esterfication LA with n-nutyl levulinate and observed that H-Beta is the most active zeolite for the reaction [53]. Acidic TiO_2 nanoparticles were used by Kuo et al for the preparation of methyl levulinate from carbohydrates and the comparision of the nanoparticles with other catayts revealed that the TiO_2 nanoparticles are better than other conventional solid acid catalysts for this conversion [54]. Mandi et al. developed Ru nanoparticles supported on mesoporos TiO_2 for esterfication and transfer hydrogenation of LA. The Ru@mesoTiO_2 catalyst was found to be stable even after five recycles [55].

In the present work, we have prepared silicalite-1 containing intracrystalline nanovoids under hydrothermal synthesis conditions by adding corn stem pith powder into the zeolite synthesis gel. The nanovoids found to increase the external surface area of the zeolite and, when HPA was supported, it was loaded onto these nanovoids which improved dispersion of HPA and accesssiblity of acid sites. X-ray photoelectron spectroscopy and ^{31}P- MAS NMR indicated interfacial bond formation between the silicalite-1 surface and HPA which would facilitate dispersion. The HPA loaded on silicalite-1 containing nanovoids and no novoids both were tested as catalysts for esterfication of levulinic acid with 1-propanol, 1-butanol and 1-heptanol. The HPA supported silicalite-1 contining nanovoids exhibited superior catalytic activity and exhibited remarkable stability even after four recycles.

2. Experimental

2.1 Materials

Tetraethylorthosilicate (98%, Sigma-Aldrich, India), tetrapropylammoniumhydroxide (1M in H_2O, Sigma-Aldrich, India), levulinic acid (98% Sigma-Aldrich, India), 1-propanol (99%, SD Fine-Chem, India), 1-butanol (99%, Sigma-Aldrich, India), 1-heptanol (99%, SD Fine-Chem, India), 12-tungstophosphoric acid hydrate (99.995%, Sigma-Aldrich, India) and poly(diallyldimethylammonium chloride) (PDDA) (20 wt% in H_2O, Sigma-Aldrich, India) were purchased and used without further purification. Corn stems piths were collected from agricultural farms located at Chettiyandhal village, Thiruvannamalai District, Tamil Nadu, India. The outer cover of the naturally dried stem pith of corn was removed and the spongy material present inside was cut into small pieces and made into fine powder using mortar and pestle after freezing it using liquid nitrogen.

2.2 Methods

2.2.1 Synthesis of silicalite-1 with intracrystalline voids

Corn stem pith powder was added to 1% poly (diallyldimethylammonium chloride) (PDDA) solution and stirred for 2 h to modify the surface charge. Then it was filtered and added into the zeolite precursor gel. In a typical synthesis, 500 mg of PDDA modified corn stem pith powder was added to a mixture containing 7 g TEOS, 8 ml TPAOH, 2 g ethanol and 2 g distilled water and stirred for 2 h. After stirring, the mixture was transferred to a Teflon lined autoclave.

The tightly closed autoclave containing the synthesis gel was kept in a hot air oven at 170 ^{o}C for 36 h. After this crystallization period, the autoclave was taken out from the hot air oven and quenched to room temperature. The solid in the autoclave was filtered, washed, dried in a hot air oven at 110 ^{o}C overnight and then calcined at 550 ^{o}C under air to remove the organic matter. The sample prepared in this manner was labelled as C-Sil-1. A silicalite-1sample without addition of corn pith powder into the zeolite precursor gel was also prepared by following the same procedure and named as Sil-1. The synthesis gel molar ratio in both the methods was 30 SiO_2: 7.3 TPAOH: 400 H_2O: 5 ETOH.

2.2.2 Supporting 12-phosphotungstic acid on zeolite

500 mg of HPA was dissolved in 10 ml of methanol and the methanolic solution was slowly added to 1000 mg of zeolite with constant string.The resulted mixture was kept overnight for stirring and then methanol was evaporated on a hot water bath. The solid was then dried in a hot air oven at 80 ^{o}C for 2h. The supported HPA catalysts prepared in this manner using C-Sil-1 and Sil-1 were labelled as HPA/C-Sil-1 and HPA/Sil-1respectively.The calculated loading of HPA on the support was ~30 wt% based on anhydrous form.

2.2.3 Catalyst characterization

A Bruker D8 advance powder X-ray diffractometer was used to record X-ray diffraction (XRD) patterns. FTIR spectra of the neat samples were recorded using Shimadu IR Affinity-1 instrument equipped with attenuated total reflection (ATR) accessory. Scanning electron microscope (SEM) images were captured using Carl Zeiss Supra-55 FESEM instrument attached with x-act EDS detector of Oxford instruments. Transmission electron microscopy (TEM) images were taken using Jeol JEM 2100 and Tecnai, G2 20 Twin TEM instruments. Nitrogen adsorption studies were carried out using a Micrometrics ASAP 2020 instrument at 77 K. Before adsorption, the samples were out gassed at 250^{o}C for 5 h. UV-Vis spectra were obtained using Jasco V-670 UV-Vis spectrophotometer equipped with an integrating sphere. The ^{31}P MAS NMR spectra were recorded on a Jeol resonance, 400 MHz NMR spectrophotometer and H_3PO_4 was used as reference. Temperature programmed desorption of NH_3 (TPD-NH_3) was performed using Quantochrome, Autosorb iQ-Chemi instrument. Before chemisorption of NH_3, the catalysts were outgassed at 500^{o}C for 1 h. After cooling down the catalyst to 100^{o}C, 20% NH_3 in He at the flow rate of 15 ml/min was passed on the catalyst for 30 min. After adsorption of NH_3,

desorption was carried out by heating the catalyst from 100 to 750^{o}C. The NH_3 desorbed was monitored using a thermal conductivity detector. X-ray photoelectron spectra was collected using a Axia Ultra (Kratos Analyticals UK) XPS instrument using Al Kα photon with 1486.6 eV energy.

2.2.4 Esterification of levulinic acid with alcohol

The esterification reaction was carried out in a double-necked RB flask fitted with a reflux condenser and $CaCl_2$ tube. 50 mmol of LA and 250 mmol of alcohol were taken in the RB flask and then heated to desired temperature using a silicone oil bath fitted with digital temperature controller and stirrer. After achieving the desired temperature, the weighed quantity of catalyst was added into the mixture. Before addition, the catalyst was pre-activated at 200 ^{o}C for 2 h under nitrogen flow and then cooled down to room temperature in a desiccator. Quantification of levulinic acid present in reaction mixture was done by using a gas chromatograph (Shimadzu GC 2010 plus, RTX-1 capillary column, length 30 m, 0.32mm ID, film thickness 0.5 µm) by internal standard method. n-Nonane was used as an internal standard and it was added into the reaction mixtures after completion of the reaction. The products were confirmed by gas chromatograph coupled with mass spectrometer (Perkin Elmer, Clarus 680 Clarus 600 (Electron ionization). The propanol ester of LA, propyl levulinate was isolated by the following procedure: The reaction mixture after filtration of the catalyst was added into 15 ml dichloromethane followed by washing with 50 ml water. The washing was repeated for three times. After washing, the contents were dried using $MgSO_4$ and then propyl levulinate was separated by evaporating the solvent using a rotary evaporator. The structure of the product, propyl levulinate was confirmed by ^{1}H and ^{13}C NMR spectra (Bruker FT-NMR 400 MHz) and GC-MS analysis. Turnover frequency (TOF) was calculated using the following formula under the conditions which give less than 50% conversion of LA as mentioned below:

TOF = Number of moles of acid sites / (moles of LA converted × reaction time in hours)

Conditions for measuring TOF values: Catalyst = HPA/Sil-1, temperature = 100 ^{o}C, 1-propanol /LA mole ratio = 5, catalyst weight = 50 mg, reaction time = 5h, conversion = 46%; Catalyst = HPA/Sil-1, temperature = 100 ^{o}C, 1-propanol/LA mole ratio = 5, catalyst weight = 100 mg, reaction time = 5 h, conversion = 31%.

3. Results and discussion

3.1 X-ray diffraction and FTIR spectroscopy

The XRD patterns of the zeolites and supported catalysts are illustrated in **Figure 1**. The prepared zeolites exhibit characteristic diffraction pattern of silicalite-1, a MFI type zeolite [56]. After supporting HPA, the original XRD patterns of the zeolites are retained indicating the zeolite structure is preserved. The diffraction peaks of bulk HPA are not observed after supporting it on zeolites probably due to dispersion and dilution of HPA by zeolites. The loading of HPA on the zeolites were confirmed by using SEM-EDX analysis and it was found to be ~35 wt% on the basis of tungsten present (Supporting information Fig.S1-S3).

The FTIR spectra of the materials are shown in **Figure 2**. The MFI structure of prepared zeolites and Keggin structure of HPA can be confirmed using FTIR spectra. In the prepared zeolites, FTIR absorption bands appear at 1220, 1075, 796 and 550 cm^{-1} which are typical of silicalite-1. The absorption bands at 1220, 1075 cm^{-1} can be correlated to external and internal asymmetric stretching vibrations of Si-O-Si. The peaks at 796 and 550 cm^{-1} can be associated to symmetric stretching of Si-O-Si and pentasil double five membered rings (D5R) vibration respectively [56,57]. The unsupported HPA shows characteristic absorption bands at 1072, 972 and 900 cm^{-1} those can be interrelated to P-O stretching, terminal W=O stretching and W-O-W asymmetric stretching of corner sharing bridged oxygens, respectively [10,11,58,59].In supported HPA catalysts, absorption bands are observed at 1070, 979, 890, 790 and 545 cm^{-1}. The band at 979 cm^{-1} could be related to terminal W=O stretching. The peaks at 890 and 790 cm^{-1} are due to W-O-W asymmetric stretching of corner sharing bridged oxygens and W-O-W asymmetric stretching of edge sharing bridged oxygens as in the case of unsupported HPA and the presence of these FTIR bands in HPA/C-Sil-1 and HPA/Sil-1 confirms the presence of Keggin anions. Since 1075 cm^{-1} band in siliclaite-1 and 1070 cm^{-1} band of HPA are overlapping they are not distinguishable in the supported catalysts. Similarly the weak band at 796 cm^{-1} in silicalite-1 is overlapping with strong absorption band of HPA at 790 cm^{-1} in the supported HPA catalysts.

3.2 Nitrogen adsorption, SEM and TEM

Nitrogen adsorption-desorption isotherms of the catalysts are shown in **Figure 3**. The isotherms are found to be type IV. In the isotherms, high uptake of nitrogen is observed in the very beginning of adsorption. This high uptake is associated with adsorption of nitrogen in micropores present in the zeolites. There are two hysteresis loops present in the isotherms of C-Sil-1 and HPA/C-Sil-1. The first hysteresis loop is observed at the relative pressure, $P/P_0 \approx 0.2$ in C-Sil-1 and the second one appeared at P/P_0 range 0.4 to 1. In Sil-1 only one hysteresis at $P/P_0 \approx 0.2$ is observed. The hysteresis at $P/P_0 \approx 0.2$ has been related to a *fluid to crystalline* like phase transition of nitrogen that occurs in MFI type zeolites, and not related to any porosity [41,60]. In the present work, when HPA is supported on the zeolites (HPA/C-Sil-1 and HPA/Sil-1) the position of the closure of adsorption and desorption branches are shifted from $P/P_0 \approx 0.2$ to $P/P_0 \approx 0.13$ hence the hysteresis is also shifted. This shift may be an indication that the loaded HPA particles present in the pores affect the pore wall-adsorbate interaction. However, still the shifted hysteresis cannot be related to porosity. The second hysteresis observed above $P/P_0 > 0.4$ is quite broad and it can be classified as H4 type hysteresis. The H4 type hysteresis is indicative of presence of slit like pores [61]. Mesoporous materials having structural defects and larger mesopores associated with much smaller pores such as micropores may also exhibit H4 type hysteresis [60]. In Sil-1 and HPA/Sil-1 H4 type hysteresis is not observed may be because of absence of additional intracrystalline porosity. The surface area and pore volume data of the prepared materials derived from N_2 adsorption isotherms are shown in **Table 1**. The Brunauer–Emmett–Teller (BET) surface area of C-Sil-1 is found to be 358 m^2/g which is higher than Sil-1 (BET surface area = 253 m^2/g) indicates that extra porosity is generated by the addition of corn stem pith powder to the precursor gel during preparation. Further it can be seen that the external surface area of C-Sil-1 (75 m^2/g) calculated using *t*-plot method is three times higher than the same of Sil-1 (25 m^2/g). The increase in total (BET) surface area and external surface area along with the presence of H4 type hysteresis indicate the formation of voids larger than micropores on surface of C-Sil-1 which may form micro/meso or

micro/macro hierarchical pores. The loading of HPA leads to decrease in micropore surface area of the zeolites which suggests that some of the micropores are blocked by HPA particles reside on the micropore mouths near the surface of zeolite. Interestingly, the external surface areas of the catalysts (HPA/C-Sil-1 = 128 m^2/g, HPA/Sil-1 = 95 m^2/g) increase after loading HPA though there is a decrease in total (BET) surface area. There is a possibility that upon loading HPA, if smaller nanoparticles on the zeolite support are formed then these particles would increase the external surface area. Hence, in order to look into surface morphology of the supports and dispersion of the supported HPA particles, SEM and TEM were employed.

The representative scanning electron microscope images of HPA/C-Sil-1 are presented in **Figure 4**. The higher magnification images of the catalyst show presence of nanovoids of different sizes on the surface. These voids are found to be absent on the Sil-1 (images not shown). These nanovoids are expected to be formed by incorporation of corn stem pith powder and its fragments generated during the synthesis conditions on the surface of zeolite crystals as proved by the authors elsewhere [42]. Corn stem pith is a cellulosic biomass capable of undergoing hydrolysis and fragmentation under basic conditions [42,62]. The incorporated lignocellulosic material, when burnt off, will leave zeolite crystals with intracrystalline nanovoids. The particle size distribution of corn pith powder used for the synthesis of zeolite was analysed using dynamic light scattering technique and the powder was found to have nanoparticles of different sizes (Supporting information Fig. S4).

The representative TEM images of Sil-1and C-Sil-1 are shown in **Figure 5**. The presence of slit like nanovoids and pores larger than micropores on the surface of zeolite crystals can be seen only on C-Sil-1 which supports our conclusion that addition of corn stem pith powder leads to the formation of nanovoids or larger pores. Transmission electron microscope images of HPA/Sil-1 and HPA/C-Sil-1 are presented in **Figure 6**. Dispersion of HPA nanoparticles (dark spots) on the surface of C-Sil-1 is evidently visible from the TEM images. In HPA/Sil-1, HPA nanoparticles seem to disperse less efficiently leading to agglomeration as sizes of many HPA particles are relatively larger than in HPA/C-Sil-1. So based on the SEM and TEM data, it is more likely that HPA upon loading resides on the surface nanovoids present on C-Sil-1 which makes it disperse more efficiently.

3.3 Temperature programmed desorption of NH_3

Temperature programmed desorption of ammonia was carried out to study acid sites present in the prepared catalysts **(Fig.7)**. The TPD traces indicate presence of two distinct desorption features in all the three catalysts. The low temperature feature is broad (170 – 400^oC) and it can be correlated to weak and medium acid sites whereas the higher temperature peaks (550 – 700 ^oC) can be related to strong acid sites [63,64].The fact that intensity of peaks related to strong acid sites decrease in intensity and the peaks are appearing at the lower temperatures in HPA/Sil-1 and HPA/C-Sil-1 compared with HPA shows that the acid sites are weakened due to supporting HPA on silicalite-1. Between HPA/C-Sil-1 and HPA/Sil-1, the shift is more in the former indicates the interaction is stronger. The previous reports indicate that in HPA supported on silica catalysts, acid strength decreases when HPA is dispersed on the support [63,64]. Newman et al. found that at lower loadings (between 5- 26 wt%), acid strength of HPA supported on silica decreases due to the interfacial bond formation between the support and HPA. The higher dispersion leads monolayer coverage of HPA on the support [65,66]. However the acid strength was found to increase when the loading was increased up to 43 wt% due to the formation of multilayer of HPA [65,66]. The total number of acid sites calculated from the amount of ammonia desorbed is 0.15 mmol/g for HPA/C-Sil-1, 0.22 mmol/g for HPA/Sil-1 and 1.24 mmol/g for HPA. The number of acid sites is lower in the supported catalysts compared to bulk HPA and this could be due to dispersion of HPA on silicalite-1 supports. In the present study, XRD patterns, N_2 adsorption data and TEM images point out possibility of better dispersion of HPA on C-Sil-1 than in Sil-1. However more detailed experiments are needed for confirmation of this assumption hence further characterization techniques were employed as follows.

3.4 UV-Vis and ^{31}P MAS NMR spectroscopy

UV-Vis spectra of the prepared materials are shown in **Figure 8**. Charge transfer absorption bands of HPA are generally observed between 200 to 400 nm in UV-Vis spectrum [67-69].Unsupported HPA has two strong absorption bands at 260 and 340 nm. These bands at 260 and 340 nm can be related to ligand (O) to metal (W) charge transfer transitions involved in edge-sharing and corner-sharing W-O-W bridges present in the Keggin units respectively [68,69] In HPA/Sil-1, the 260 nm absorption is retained but the 340 nm band intensity decreases and it

appears as a shoulder. In HPA/C-Sil-1, the band at 260 nm remains unchanged whereas the band at 340 nm is blue shifted. The absorption band at 260 nm is retained in both the HPA supported samples which shows this particular transition is not affected while supporting HPA on the zeolites. The blue shift and intensity loss of 340 nm peak indicates that supporting HPA on zeolite affects the associated charge transfer. When HPA loading is decreased from 100 (unsupported) to 30, 20 and 10 wt%, the absorption edge found to blue shift (results of 10 and 20 wt% are not shown) due to quantum confinement effect as at lower loadings, the particle size would be reduced. If HPA is dispersed on zeolite then there might be some interaction of the support with HPA and it will affect the Keggin unit's ligand environment. As reported before, the interaction of Keggin units with zeolite and the resulted changes in dispersion of HPA can alter the acidity and activity of the catalyst [21, 22, 71].

The ligand environment of Keggin units can be visualized through ^{31}P-MAS NMR spectra (**Figure 9)**. In unsupported HPA, two sharp resonance peaks are observed at -15.2 and -14.9 ppm. In HPA, depending on hydration level, the resonance peaks may appear anywhere from -12 to -16 ppm and a down field shift is observed when HPA undergoes dehydration [21]. In the present work, the peak observed at -15.2 ppm in unsupported HPA can be correlated to fully hydrated (hexahydrate) Keggin units and the one observed at -14.9 ppm may be related to the Keggin units undergone some degree of dehydration during sample preparation or analysis. In HPA/Sil-1, there are three resonance peaks observed at -15.2, -14.9 and -14.6 ppm. The intensity of -14.9 ppm peak in HPA/Sil-1 is higher than -15.2 ppm peak which is reverse of the observation in unsupported HPA. In the case of HPA/C-Sil-1, only two resonance peaks at -14.9 and -14.6 ppm are observed. The -15.2 ppm peak is completely absent in HPA/C-Sil-1. These observations indicate that the ligand environment of Keggin units in the supported HPA is considerably different from unsupported HPA and Keggin units undergo more degree of dehydration when it is interacting with the supports [21,72,73]. It has been postulated that when HPA is supported on silica based supports, it may react with the hydroxylated surface to form ion pair with one or more silanol groups via proton transfer involving dehydration [21,65,74] Based on these previous reports we presume that the resonance peaks observed at -14.9 and -14.6 ppm are more likely related to HPA interacting with surface silanol groups present in two different locations probably external surface or nanovoids and pore mouths of micropores of zeolites respectively. The fact that the -15.2 peak is present with reduced intensity on HPA/Sil-1

shows the presence of both fully hydrated, Keggin units of bulk HPA particles not interacting with the support and the ones interacting with the support (-14.9 and -14.6 ppm peaks). The absence of -15.2 ppm peak in HPA/C-Sil-1 indicates that Keggin units are well dispersed on C-Sil-1 so that the unsupported, fully hydrated Keggin units are not present. This variation between HPA/C-Sil-1 and HPA/Sil-1 may arise because of differece in the textural properties of the supports. In C-Sil-1, the external surface area is more because of the presence of nanovoids or pores larger than micropores on the surface of the silicalite-1 crystals. So when HPA is loaded on C-Sil-1, it will interact more with the surface of the support than in the case of Sil-1which possess no such voids or larger pores.

3.6 X-ray photoelectron spectroscopy

Nuclear magnetic resonance spectroscopy (^{31}P-MAS NMR) is not a surface sensitive technique so it cannot give a conclusive evidence for the interaction of the support with HPA. Hence, XPS, which is a surface sensitive technique, was employed for this purpose. The W4f XPS spectra of unsupported HPA and HPA/C-Sil-1 are shown in **Figure 10**. In both samples, typical broad doublets centered at binding energies, 38.2 and 36 eV, related to $4f_{5/2}$ and $4f_{7/2}$ respectively [73,75-76] are observed. Upon deconvolution of the $4f_{7/2}$ component, Newman et. al. observed bands at 35.3 and 33.8 eV on HPA supported SiO_2. The authors correlated the 35.3 eV band to bulk HPA and the low energy 33.8 eV band to a perturbed tungstate environment in the interface between HPA and SiO_2 [73]. Jalil et al. correlated the shoulder obtained at lower binding energy, 34.3 eV on the $4f_{7/2}$ band to water molecules surrounding Keggin units [75]. Legagneux et al. did not observe any lower energy shoulder in the W4f spectra while studying silica supported HPA as s function of dihydroxylation temperature [76]. In the present work, deconvolution of the $4f_{7/2}$ band resolved it into different bands as shown in the insets. In the case of HPA/C-Sil-1, a lower binding energy band at 35.3 eV could be observed which is absent in HPA. We correlate this lower energy band to interfacial tungstate species as proposed by Newman et al. Presence of this interfacial tungstate species proves that HPA indeed have strong interaction with zeolite surface.

3.7 Esterification of levulinic acid

The prepared catalysts were tested for esterification of levulinic acid (LA) with different alcohols at the same reaction conditions. The reactions were also conducted in the absence of any catalyst and over unsupported HPA for comparison. In all the reactions, high alcohol to LA ratio (5:1) was maintained to facilitate the forward reaction. The conversions of LA with different alcohols and selectivity of the esters obtained over different catalysts are shown in Table 2. In the absence of catalyst, LA conversion was only between 10 to 13%. Introduction of Sil-1 and C-Sil-1 as catalysts improved LA conversion only slightly. Between the two supported HPA catalysts, when HPA/C-Sil-1 was employed, the conversion of LA enhanced more remarkably. The conversions of 1-propanol, 1-butanol and 1-heptanol were 90, 93 and 76% respectively over HPA/C-sil-1 whereas with HPA/Sil-1, the conversions were 31, 29 and 34%. The esterification reactions were also performed using 35 mg of bulk HPA which is equal to that of HPA present in 30wt% HPA/C-Sil-1 and found that the conversion of levulininc acid (38%) was much lower than 30wt% HPA/C-Sil-1. Further bulk HPA dissolved in the reaction medium and could not be separated after the reaction. Turnover frequency (TOF) was calculated for the reaction of LA with 1-propanol under the reaction conditions yielding less than 50% LA conversion as mentioned elsewhere in the manuscript. The TOF values of HPA/C-Sil-1 and HPA/Sil-1 were 558 and 141 h^{-1}, respectively. Comparison of the TOF values indicates that turnover of the molecules per active site is more in HPA/C-Sil-1 than HPA/Sil-1. The enhancement of catalytic activity found in the case of HPA/C-sil-1 is in agreement with the physicochemical characterization results discussed above. Due to the intracrystalline nanovoids present on the support, which leads to higher dispersion HPA, active sites (or acid sites) are more easily accessible in HPA/C-Sil-1 than in HPA/Sil-1 making HPA/C-Sil-1 more active catalyst. Propyl levulinate obtained in the reaction was separated and its structure was confirmed using NMR spectroscopy (Supporting information Fig.S.5-S.8). The results indicated presence of intracrystalline nanovoids, higher external surface area and better dispersion of HPA in HPA/C-Sil-1which may expose more accessible acid sites to the reactants. The better catalytic efficiency of HPA/C-Sil-1 is in line with the previous reports showing the advantage of using mesoporous or hierarchical zeolites as a support for HPA [4,21,22].

The study was further extended to investigate the influence of reaction time, catalyst weight and temperature on LA conversion taking the reaction of LA with 1-propanol over HPA/C-Sil-1 as an example. The reaction was conducted for 1, 3, 5 and 8 h and conversion of

LA was monitored **(Fig.11)**. The conversion found to increase from 1 to 5 h and reach 90 % at 5h. Further increasing reaction time to 8 h decreased LA conversion to 78%. This decrease in conversion may be due to the reverse reaction i.e. hydrolysis of the ester which is also an acid catalysed reaction. The reaction was tested by varying the catalyst weight. As seen in **Figure 12** increasing catalyst weight had a positive influence on conversion of LA which affirmed the role of catalyst in the reaction. The influence of temperature on LA conversion was investigated by carrying out the reaction at 30, 70 and 100 ^{o}C **(Fig. 13)**. Increasing temperature had a positive influence on LA conversion.

3.7 Reusability of the catalyst

The reusability of HPA/C-Sil-1 was studied in the reaction between levulinic acid and 1-propanol for four recycles under the optimized experimental conditions **(Fig.14)**. After completion of each cycle, the catalyst was filtered and washed with 1- propanol, dried and then used in the next cycle. Even after four repeated use, the conversion of LA was found to remain the same showing the stable nature of the catalyst and further indicating absence of HPA leaching. The aliquot after the reaction was checked for tungsten leached from HPA by using UV-Vis spectroscopy as reported by other researchers and no leaching was observed [77]. SEM-EDX analysis of HPA/C-Sil-1 showed that HPA is retained on the support even after four recycles as there is no leaching (Supporting information Fig.S3). Further, the supported HPA nanoparticles could be seen in TEM images of HPA/C-Sil-1 after four recycles which once again confirmed the stability of the catalyst (Supporting information Fig.S9). At the same time, when HPA/Sil-1 was recycled under similar reaction conditions, the conversion found to decrease from 31% on the fresh catalyst to 5% on the three times recycled catalyst (Supporting information S10). The stability of the HPA/C-Sil-1 catalyst could be linked to strong interaction of HPA with C-Sil-1 leading to its higher dispersion as indicated by various characterization results discussed above.

Conclusion

Silicalite-1 with intracrystalline nanovoids could be prepared by adding corn pith powder, an agricultural waste into the zeolite synthesis gel. This zeolite with intracrystalline nanovoids acts as a better support for HPA than scilicalite-1 as it interacts with HPA and makes it disperse

well leading to the acid sites of HPA more accessible. The HPA supported on silicalite-1 containing nanovoids acts as the better catalyst for esterification of levulinic acid with 1-propanol, 1-butanol and 1-heptanol than HPA supported on silicalite-1 containing no nanovoids. The interaction of HPA with zeolite support makes it a stable catalyst even after four times of recycling.

Acknowledgement

This work was funded by Science and Engineering Research Board (SERB), Department of Science and Technology, New Delhi, India (Sanction No: SR/FT/CS-65/2011). The authors thank NMR facility, Indian Institute of Science, Bengaluru for ^{31}P-MAS NMR analysis, Sophisticated Instruments Facility (SIF) of VIT University, Vellore for ^{1}H-NMR, ^{13}C-NMR, GC-MS, XRD and TEM analysis, Amrita Center for Nanosciences and Molecular Medicine, Kochin, India for XPS data and IIT Madras for TPD of ammonia and N_2 adsorption. The author K. Manikandan is grateful to VIT University, Vellore for research fellowship.

References

[1] E. Rafiee, F. Shahbazi, J. Mol. Catal. A Chem. 250 (2006) 57–61.

[2] B. Rác, G. Mulas, A. Csongrádi, K. Lóki, Á. Molnár, Appl. Catal. A Gen. 282 (2005) 255–265.

[3] S. Wu, J. Wang, W. Zhang, X. Ren,Catal. Letters. 125 (2008) 308–314.

[4] Chengyi Dai, Anfeng Zhang, Junjie Li, Keke Hou, Min Liu, and X. Guo, Chem. Commun. 50 (2014) 4846–4848.

[5] E. Rafiee, F. Shahbazi, M. Joshaghani, F. Tork, J. Mol. Catal. A Chem. 242 (2005) 129–134.

[6] B.M. Devassy, S.B. Halligudi, J. Catal. 236 (2005) 313–323.

[7] T. Blasco, A. Corma, A. Martinez, P. Martinez-Escolano, J. Catal.177 (1998) 306–313.

[8] G.Satish Kumar, M. Vishnuvarthan, M. Palanichamy, V. Murugesan, J. Mol.Catal. A: Chem. 260 (2006) 49–55.

[9] K.U. Nandhini, B. Arabindoo, M. Palanichamy, V. Murugesan, J. Mol. Catal. A Chem. 223 (2004) 201–210.

[10] L.R Pizzio, P.G Vázquez, C.V Cáceres, M.N Blanco, Appl. Catal. A Gen. 256 (2003) 125–139.

[11] F.J. Méndez, A. Llanos, M. Echeverría, R. Jáuregui, Y. Villasana, Y. Díaz, G. Liendo-polanco, M.A. Ramos-garcía, T. Zoltan, J.L. Brito, Fuel. 110 (2013) 249–258.

[12] Yuanhang Ren, B. Yue, Min Gu, Heyyang He, Materials. 3 (2010) 764–785.

[13] Sa-Sa Wang, Guo-YuYang, Chem. Rev. 115 (2015) 4893–4962.

[14] A.S. Badday, A.Z. Abdullah, K. Lee, Renew. Energy 62 (2014) 10–17.

[15] Y.I.K. Urabe, Chem. Lett. (1981) 663–666.

[16] P. Ferreiraa, I.M. Fonsecab, A.M. Ramosb, J. Vitalb, J.E. Castanheiro, Catal. Commun. 12 (2011) 573–576.

[17] A. Jha, A.C. Garade, S.P. Mirajkar, C.V.Rode, Ind. Eng. Chem. Res. 51 (2012) 3916–3922.

[18] F. Marme, G. Coudurier, J.C. Vedrine, Microporous Mesoporous Mater. 22 (1998) 151–163.

[19] G.D. Yadav, P.A. Chandan, N. Gopalaswami, Clean Technol. Environ. Policy. 14 (2012) 85–95.

[20] T. Chen, Y. cheng Che, Y. Zhang, J. min Zhang, F. Wang, Z. zhen Wang, J. Porous Mater. 21 (2014) 495–502.

[21] K. Zhu, J. Hu, X. She, J. Liu, Z. Nie, Y. Wang, C.H.F. Peden, J.H. Kwak, J.Am.Chem.Soc. 131 (2009) 9715–9721.

[22] K.Y. Nandiwale, S.K. Sonar, P.S. Niphadkar, P.N. Joshi, S.S. Deshpande, V.S. Patil, V. V Bokade, Appl. Catal. A: Gen. 460-461 (2013) 90–98.

[23] A.S. Golezani, A.S. Fateh, H.A. Mehrabi, Prog. Nat. Sci. Mater. Int. 26 (2016) 411–414.

[24] Z. Le Hua, J. Zhou, J.L. Shi, Chem. Commun. 147 (2011) 10536–10547.

[25] D. P. Serrano, J. M. Escola, P. Pizarro, Chem. Soc. Rev. 42 (2013) 4004–4035.

[26] K. Moller, B. Yilmaz, U. Muller, T. Bein, Chem. Mater. 23 (2011) 4301–4310.

[27] Kyungsu Na, Changbum Jo, Jeongnam Kim, Kanghee Cho, Yongbeom Seo, Robert J. Messinger, Science 333 (2011) 328-332.

[28] Feng-shou Xia, LifengWang, Chengyang Yin, Kaifeng lin, yan Di, Jixue li, Ruren Xu, Dang sheng su, Robert schogl , Toshiyuki yokoi, Takashi Tatsumi, Angew.Chem. Int. Ed. 45 (2006) 3090–3093.

[29] C. Madsen, C.J.H. Jacobsen, Chem. Commun. 673 (1999) 673–674.

[30] I. Schmidt, A. Krogh, K. Wienberg, A. Carlsson, M. Brorson, Class J.H.Jacobsen, Chem. Commun. (2000) 2157–2158.

[31] J. B. Koo, N. Jiang, S. Saravanamurugan, M. Bejblová, Musilová, Zuzana, Jiri cejka, S. E. park, J.Catal. 276 (2010) 327–334.

[32] R. Chal, C. Gorardin, M. Bulut, S. Van Donk, ChemCatChem. 3 (2011) 67–81.

[33] P.J. Kooyman, P. Van Der Waal, H. Van Bekkum, Zeolites. 18 (1997) 50–53.

[34] M. Ogura, S. Shinomiya, J. Tateno, Y. Nara, M. Nomura, E. Kikuchi, M, Appl. Catal. A Gen. 219 (2001) 33–43.

[35] V.P. Valtchev, M. Smaihi, A. C. Faust, Loic Vidal, Chem. Mater. 16 (2004) 1350–1355.

[36] V. Valtchev, F. Gao, L. Tosheva, New J.Chem. 32 (2008) 1331–1337.

[37] A. Dong, Y. Wang, Y. Tang, N. Ren, Y. Zhang, Y. Yue, Z. Gao, Adv. Mater. 14 (2002) 926–929.

[38] B.T. Holland, L. Abrams, A. Stein, J.Am.Chem.Soc. 121 (1999) 4308–4309.

[39] Y.J. Lee, J.S. Lee, Y.S. Park, K.B. Yoon, Adv. Mater. 13 (2001) 1259–1263.

[40] W. Cui Li, A. H. Lu, R. Palkovits, W. Schmidt, B. Spliethoff, Ferdi Schuth, J.Am.Chem.Soc. 127 (2005) 12595–12600.

[41] Bin Li, Zhijie Hu, Biao Kong, Jinxiu Wang, Wei Li, Zhenkun Sun, Xufang Qian, Wei Shen, Hualong Xu, and D.Xhao, Chem. Sci. 5 (2014) 1565–1573.

[42] M. Krishnamurthy, K. MSM, C.K. Krishnan, Microporous Mesoporous Mater. 221 (2016) 23–31.

[43] Y. Kuwahara, W. Kaburagi, K. Nemoto, T. Fujitani, Applied Catal. A, Gen. 476 (2014) 186–196.

[44] J.N. Chheda, G.H.Huber, J.A. Dumesic, Angew.Chem. Int. Ed. 46 (2007) 7164–7183.

[45] K. Yan, C. Jarvis, J. Gu, Y. Yan, Renew. Sustain. Energy Rev. 51 (2015) 986–997.

[46] B. Banerjee, R. Singuru, S.K. Kundu, K. Dhanalaxmi, L. Bai, Y. Zhao, B.M. Reddy, A. Bhaumik, J. Mondal, Catal. Sci. Technol. 6 (2016) 5102–5115.

[47] C. Ortiz-cervantes, M. Flores-alamo, J.J. Garc, ACS Catal. 5 (2015) 1421–1431.

[48] W. Luo, M. Sankar, A.M. Beale, Q. He, C.J. Kiely, P.C.A. Bruijnincx, B.M. Weckhuysen, Nat. Commun. 6 (2015) 6450.

[49] X. Kong, S. Wu, X. Li, J. Liu, Energy Fuels. 30 (2016) 6500–6504.

[50] S. Dharne, V. V. Bokade, J. Nat. Gas Chem. 20 (2011) 18–24.

[51] A. V Nakhate, G.D. Yadav, ACS Sustain. Chem. Eng. 4 (2016) 1963–1973.

[52] M.A. Tejero, E. Ramírez, C. Fité, J. Tejero, F. Cunill, Appl. Catal. A Gen. 517 (2016) 56–66.

[53] K. Maheria C, J. Kozinski, A. Dalai, Catal. Letters 143 (2013) 1220–1225.

[54] C.H. Kuo, A.S. Poyaraz, L. Jin, Y. Meng, L. Pahalagedara, S.Y. Chen, D.A. Kriz, C. Guild, A. Gudz, steven L. Suib, Green Chem. 16 (2014) 785–791

[55] U. Mandi, N. Salam, S.K. Kundu, A. Bhaumik, S.M. Islam, RSC Adv. 6 (2016) 73440–73449.

[56] M.S.M. Kamil, K. Manikandan, S.P. Elangovan, M. Ogura, K.K. Cheralathan, Indian J. Chem. Sect. A. 54A (2015) 469–477.

[57] Li C and Wu Z, Hand book of zeolite science and technology (Marcel Dekker Inc, New York), 2003.

[58] P.A. Jalil, M.A. Al-daous, A.A. Al-arfaj, A.M. Al-Amer, J. Beltramini, S.A.I. Barri, Appl. Catal. A Gen. 207 (2001) 159–171.

[59] J. Haber, K. Pamin, L. Matachowski, D.Mucha, Appl. Catal. A Gen. 256 (2003) 141–152.

[60] H. Li, Y. Sakamoto, Z. Liu, T. Ohsunad, O. Terasaki, M. Thommese, S.Che, Microporous Mesoporous Mater. 106 (2007) 174–179.

[61] Y.W. An-Hui Lu, Dongyuan Zhao, Nanocasting: A Versatile Strategy for Creating Nanostructured Porous Materials, RSC Nanoscience & Nanotechnology, 2009.

[62] H.P.S.A. Khalil, A.H. Bhat, A.F.I. Yusra, Carbohydr. Polym. 87 (2012) 963–979.

[63] M.H. Bhure, I. Kumar, A.D. Natu, R.C. Chikate, C. V Rode, Catal. Commun. 9 (2008) 1863–1868.

[64] A. Jha, A.C. Garade, S.P. Mirajkar, C. V Rode, Indusrial Eng. Chem. Reasearch 51 (2012) 3916–3922.

[65] A.D. Newman, D.R. Brown, P. Siril, F. Lee, K. Wilson, Phys.Chem.Chem.Phys. 8 (2006) 2893–2902.

[66] A.D. Newman, A.F. Lee, K. Wilson, N.A. Young, Catal. Letters 102 (2005) 45–50.

[67] G. Ranga Rao, T. Rajkumar, Catal. Letters. 120 (2008) 261–273.

[68] K.U. Nandhini, B. Arabindoo, M. Palanichamy, V. Murugesan, J. Mol. Catal. A Chem. 243 (2006) 183–193.

[69] M. Wu, Q.Q. Zhao, J. Li, X. Li Su, H.Y. Wu, X.X. Guan, X.C. Zheng, J. Porous Mater. 23

(2016) 1329–1338.

[70] K.U. Nandhini, J.H. Mabel, B. Arabindoo, M. Palanichamy, V. Murugesan, Microporous Mesoporous Mater. 96 (2006) 21–28.

[71] H. Suk Yun, M. Kuwabara, J. Mater. Sci. 39 (2004) 2341 – 2347.

[72] A. Ghanbari-Siahkali, A. Philippou, J. Dwyer, M.W. Anderson, Appl. Catal. A Gen. 192 (2000) 57–69.

[73] I. V Kozhevnikov, A. Sinnema, R.J.J. Jansen, K. Pamin, H. Vanbekkum, Catal. Letters. 30 (1995) 241–252.

[74] T. Blasco, A. Corma, A. Mart, P. Mart, J. Catal. 177 (1998) 306–313.

[75] P.A. Jalil, M. Faiz, N. Tabet, N.M. Hamdan, Z. Hussain, J. Catal. 217 (2003) 292–297.

[76] N. Legagneux, J. Basset, A. Goguet, C. Hardacre, Dalt.Trans. (2009) 2235–2240.

[77] G.D. Yadav, N.Kirthivasan, Appl. Catal. A Gen. 154 (1997) 29–53.

Figure captions:

Fig.1. XRD patterns of supports and catalysts (inset is the pattern of HPA)

Fig.2. FTIR spectra of supports and catalysts

Fig.3. Nitrogen adsorption and desorption isotherms of supports and catalysts (data of HPA/C-Sil-1 was offset to 5 cc/g higher)

Fig.4. SEM images of HPA/C-Sil-1

Fig.5. TEM images of Sil-1 and C-Sil-1

Fig.6. TEM images of catalysts (a) & (b) HPA/C-Sil-1 and (c) & (d) HPA/Sil-1

Fig.7. TPD of ammonia traces of catalysts (a) HPA/C-Sil-1 (b) HPA/Sil-1 (c) HPA

Fig.8. UV-Vis spectra of supports and catalysts

Fig.9. ^{31}P-MAS NMR spectra of catalysts

Fig.10. X-ray photoelectron spectra of catalysts (a) HPA (b) HPA/C-Sil-1

Fig.11. Effect of time on levulinic acid conversion over HPA/C-Sil-1 (Temperature = 100 ^{o}C, 1-propanol: LA mole ratio = 5:1, catalyst weight = 100 mg)

Fig.12. Effect of catalyst weight on levulinic acid conversion (Catalyst = HPA/C-Sil-1 Temperature = 100 ^{o}C, 1-propanol: LA mole ratio = 5:1, time = 5h)

Fig.13. Effect of temperature on levulinic acid conversion (Catalyst = HPA/C-Sil-1, 1-propanol : LA mole ratio = 5:1, time = 5h, catalyst weight = 100 mg)

Fig.14. Recycling of HPA/C-Sil-1 (temperature = 100 ^{o}C, 1-propanol: LA mole ratio = 5:1, catalyst weight = 100 mg; reaction time = 5 h)

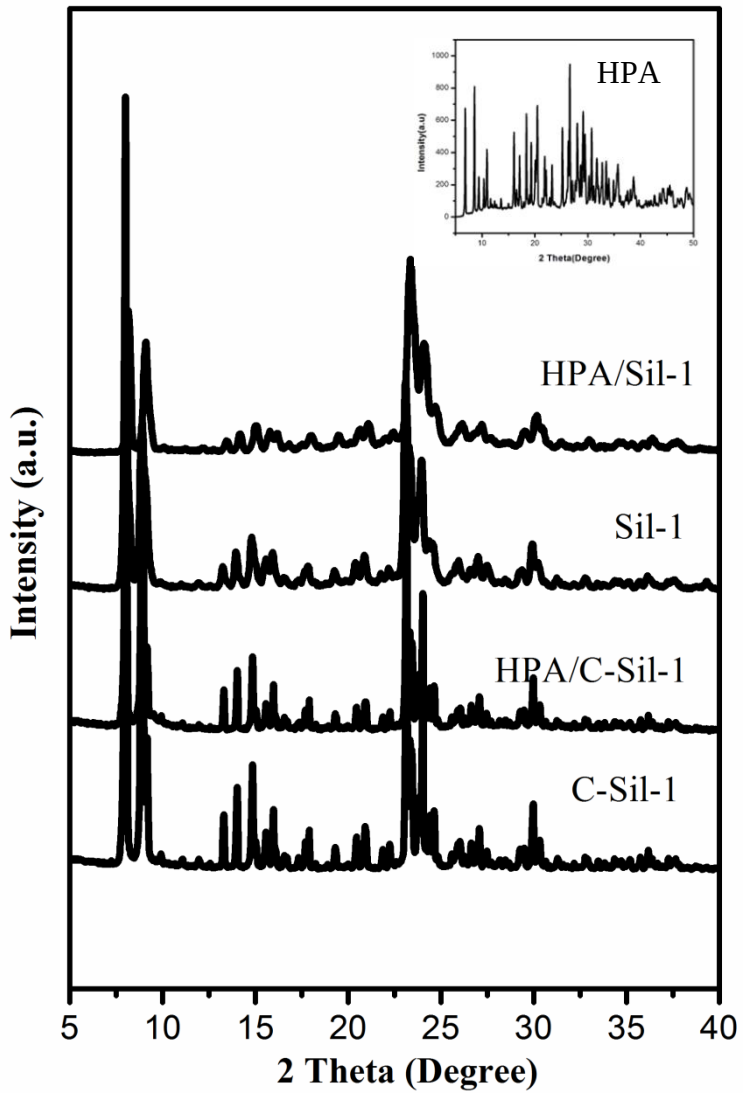

Fig 1

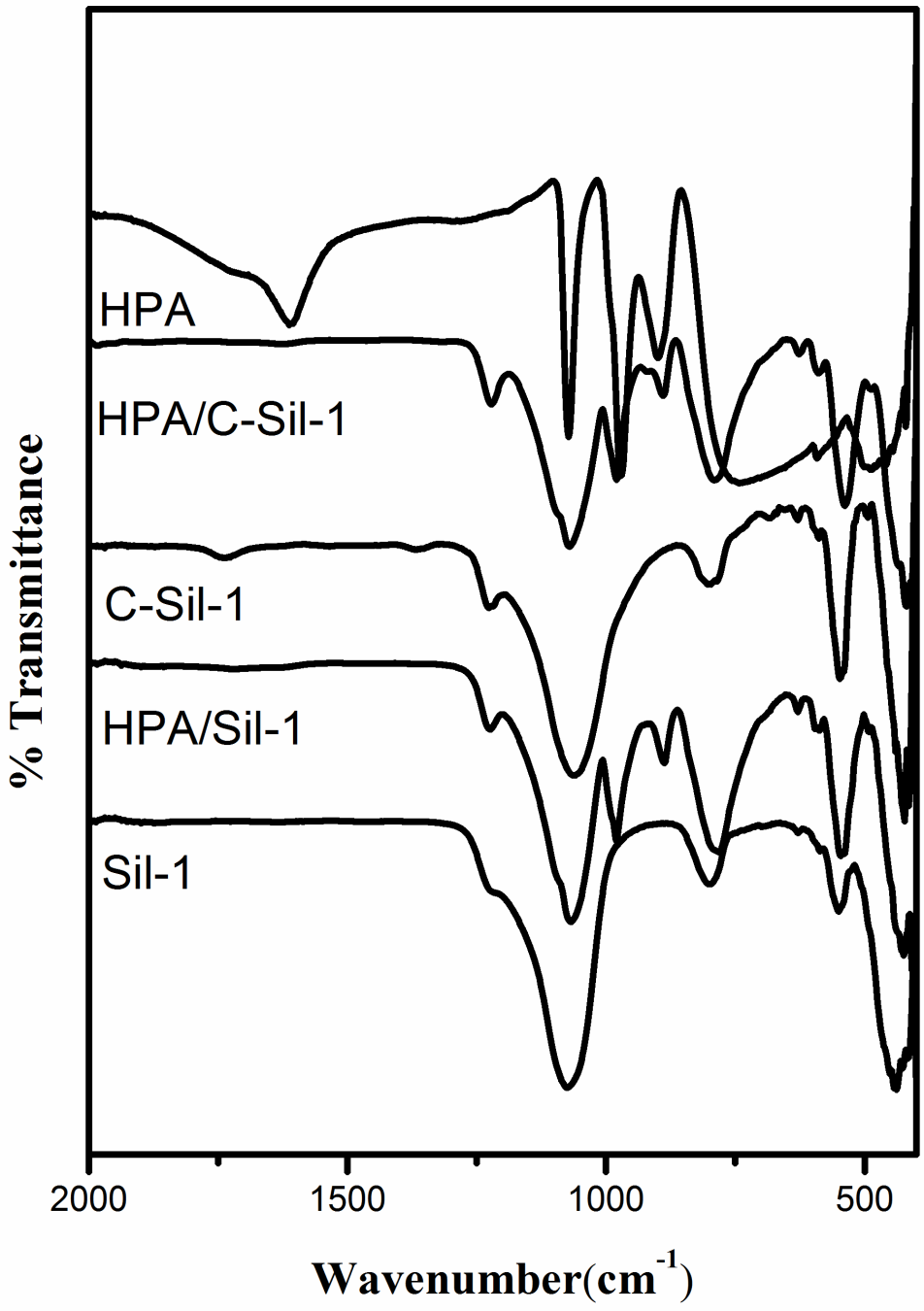

Fig 2

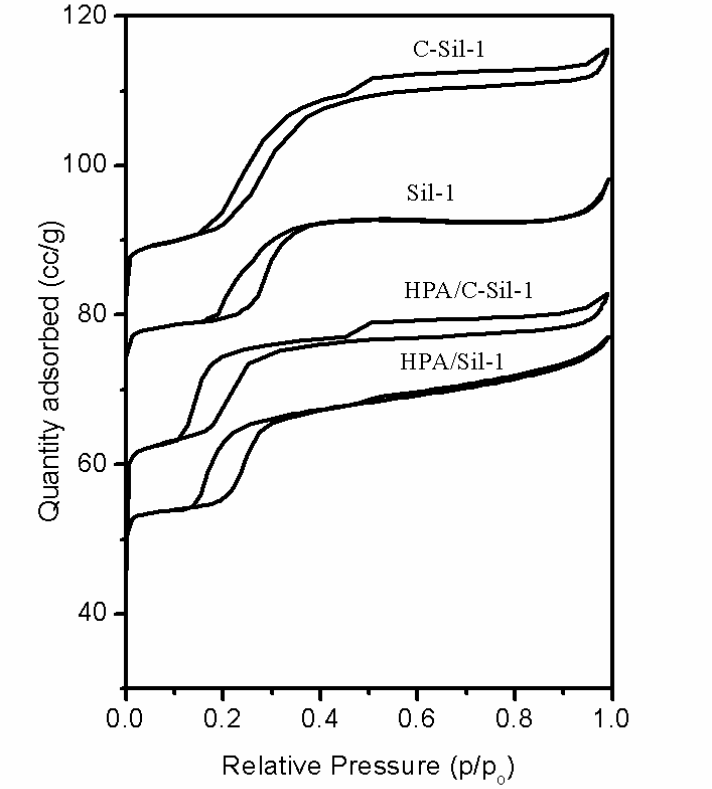

Fig 3

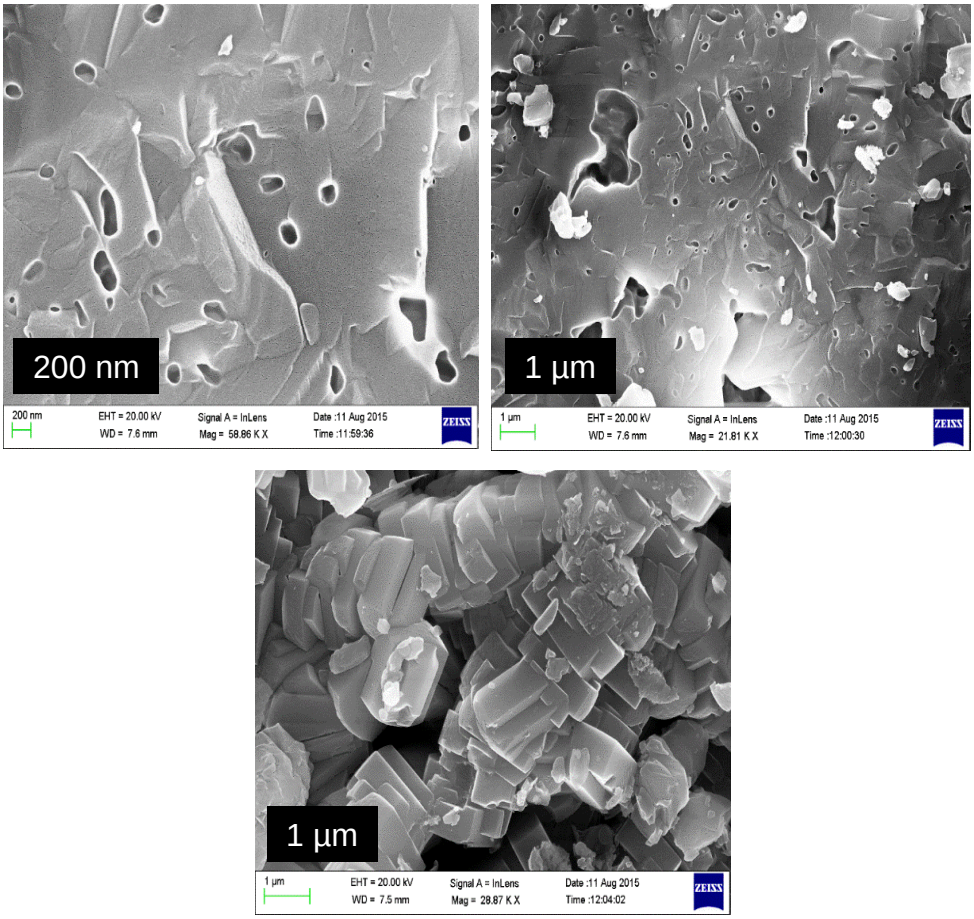

Fig.4

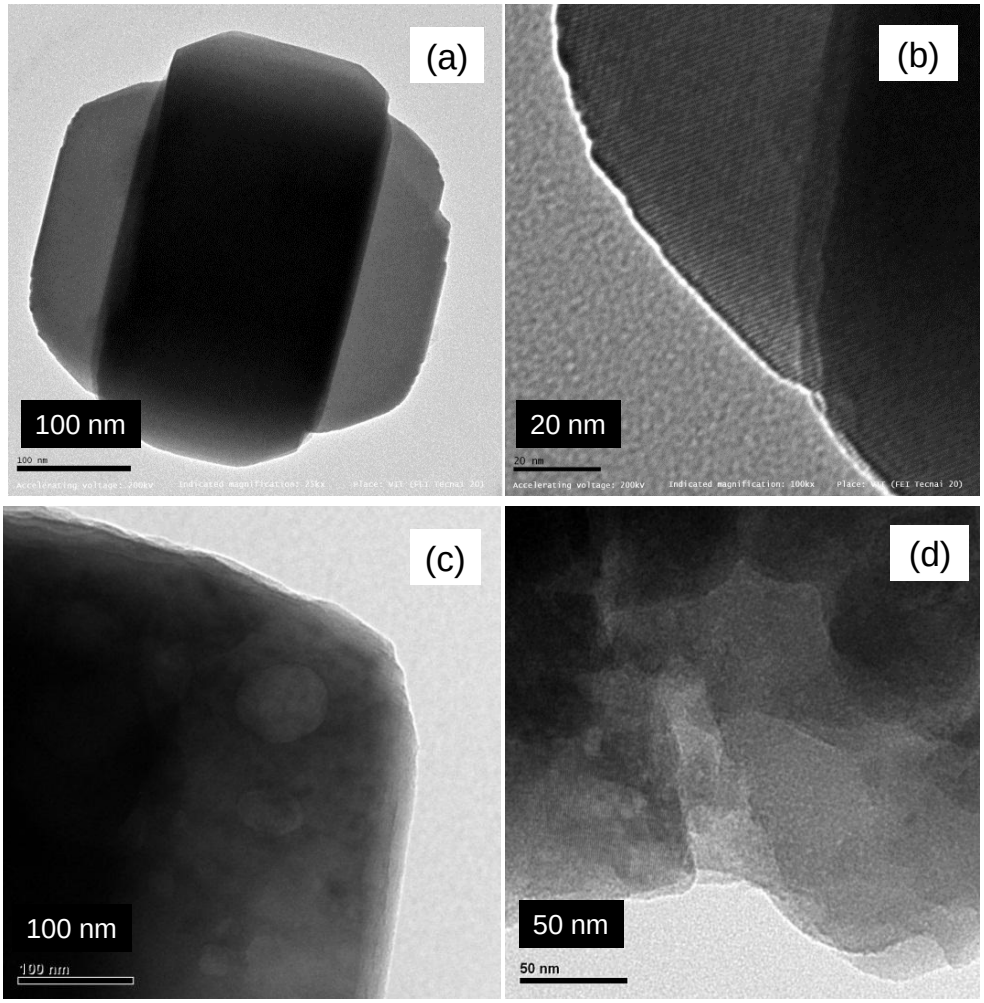

Fig.5

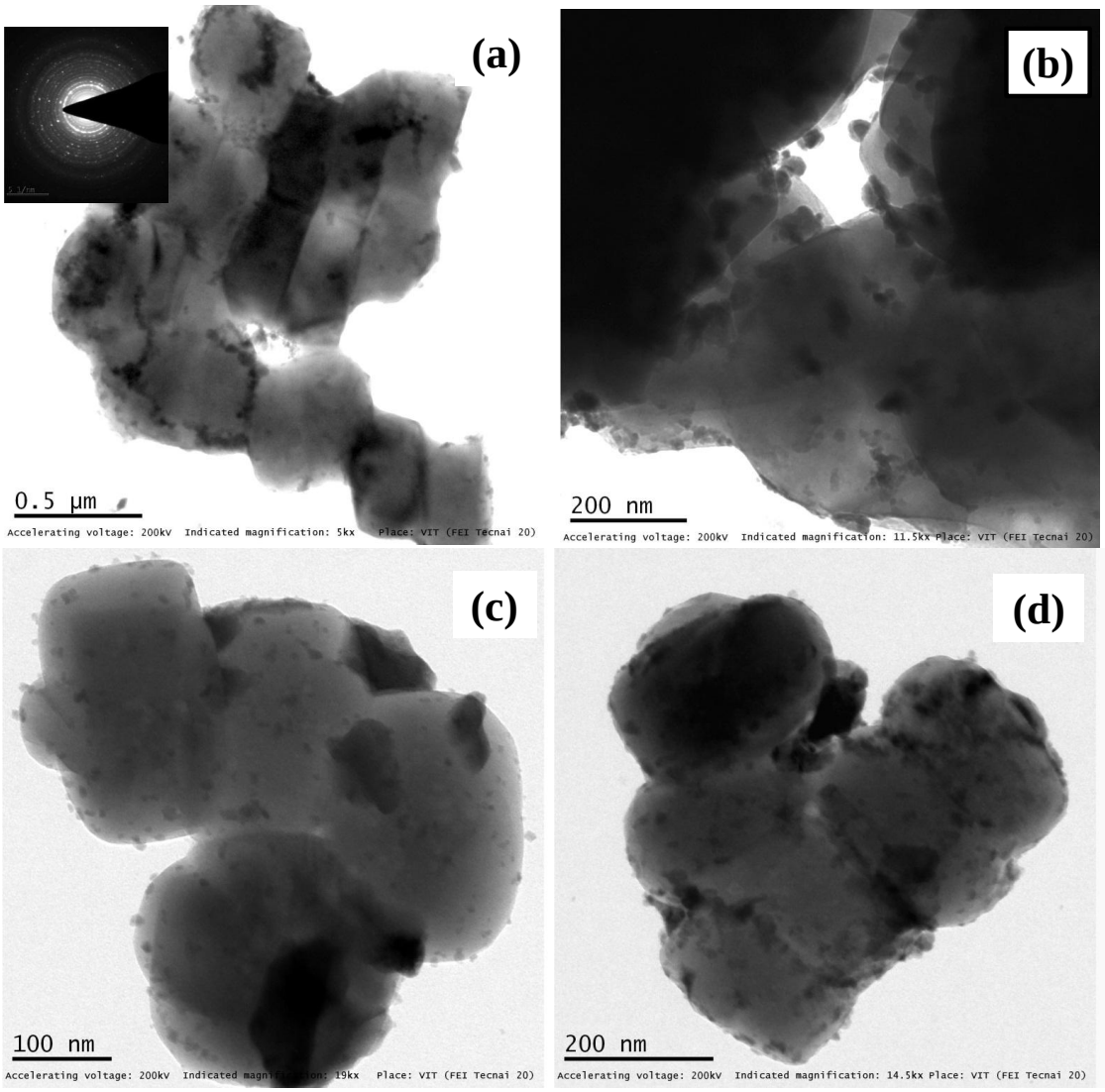

Fig.6

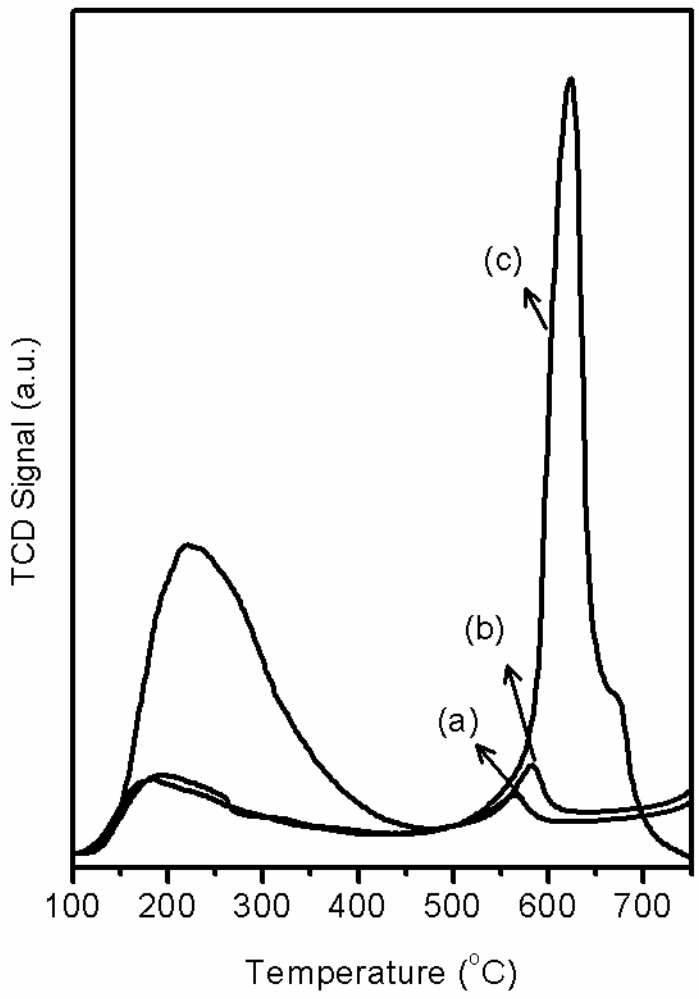

Fig.7

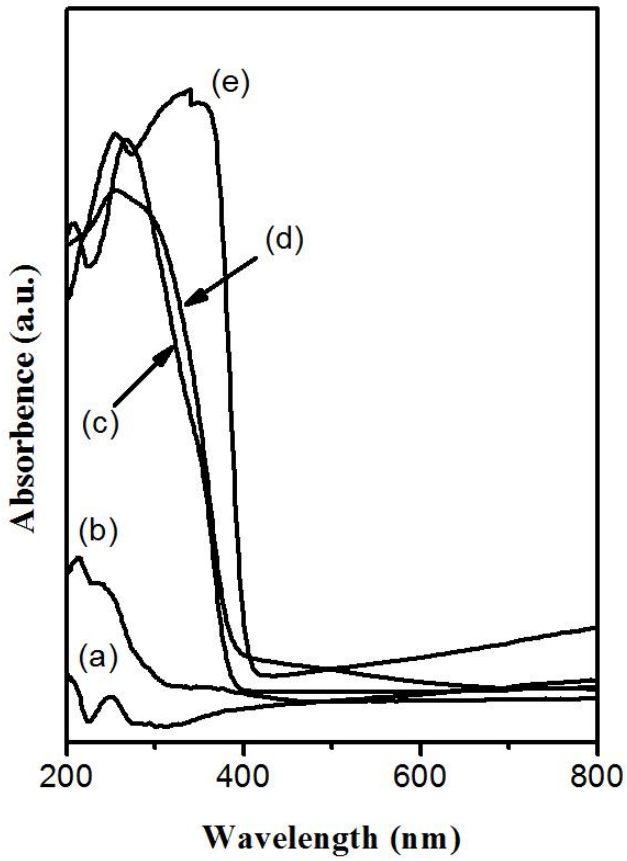

Fig.8

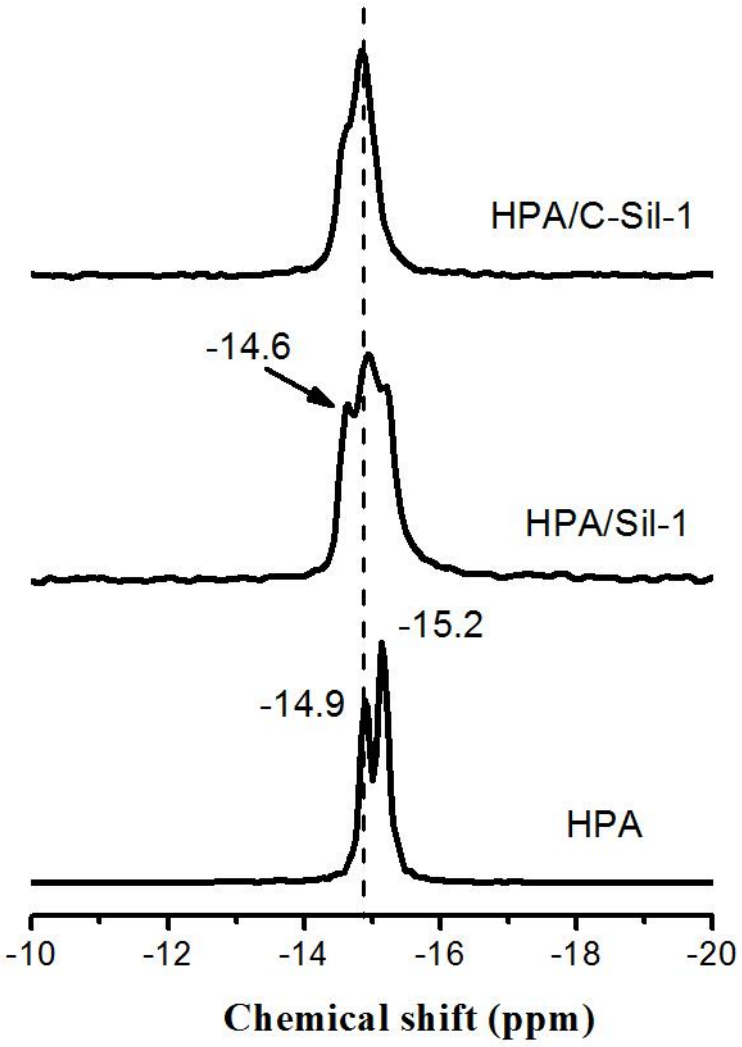

Fig.9

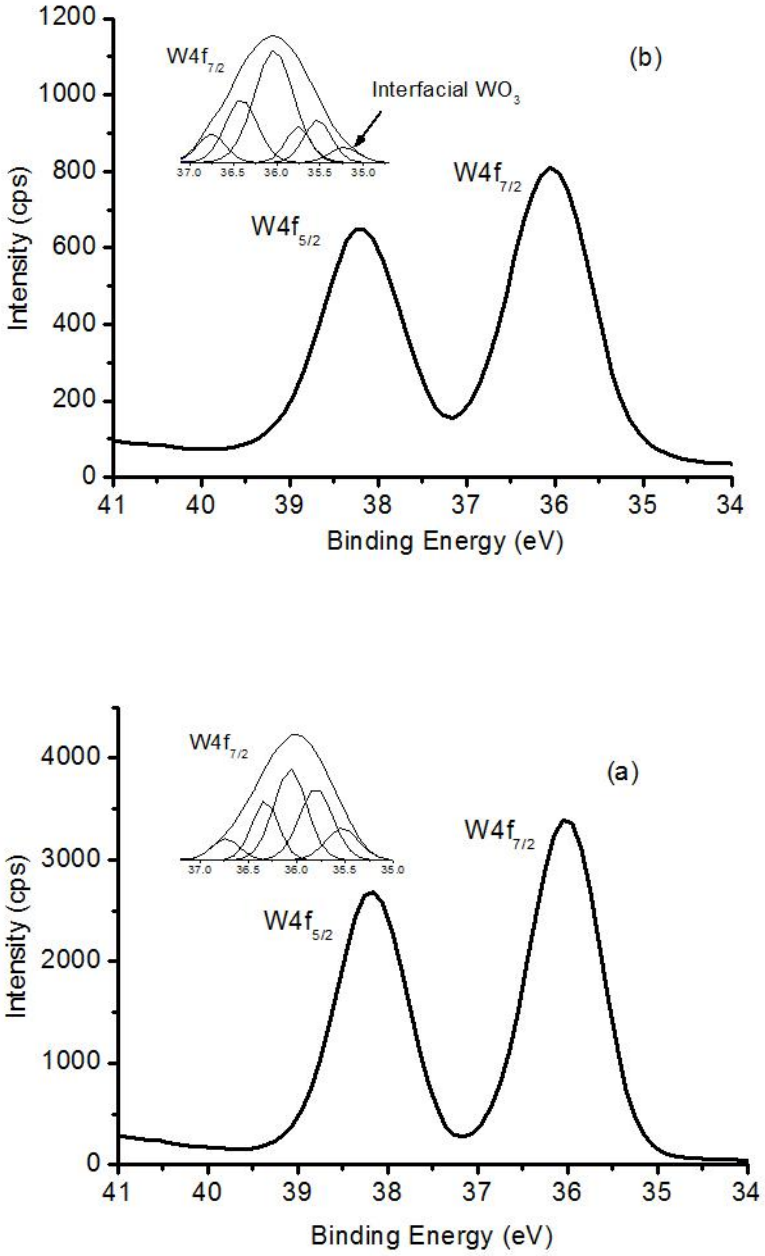

Fig.10

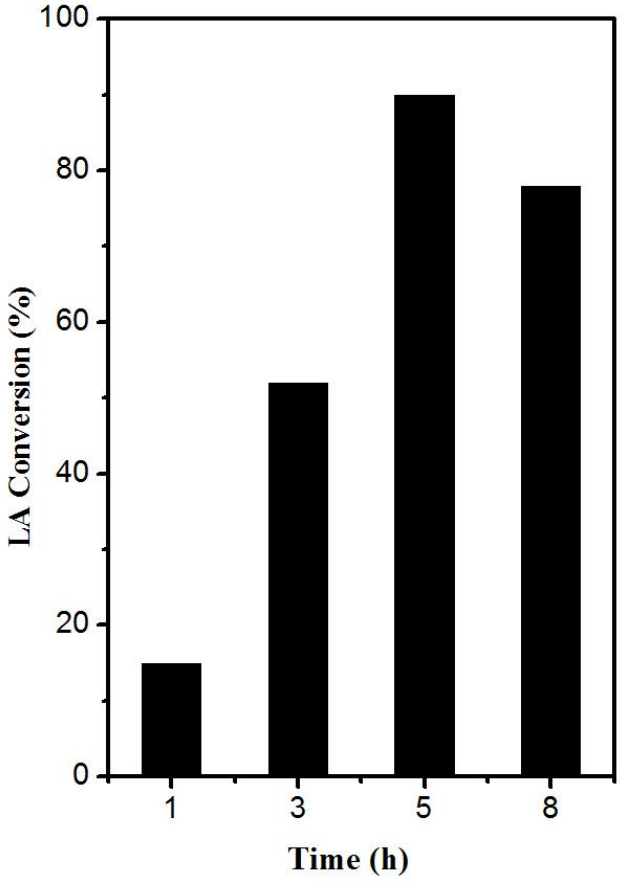

Fig.11.

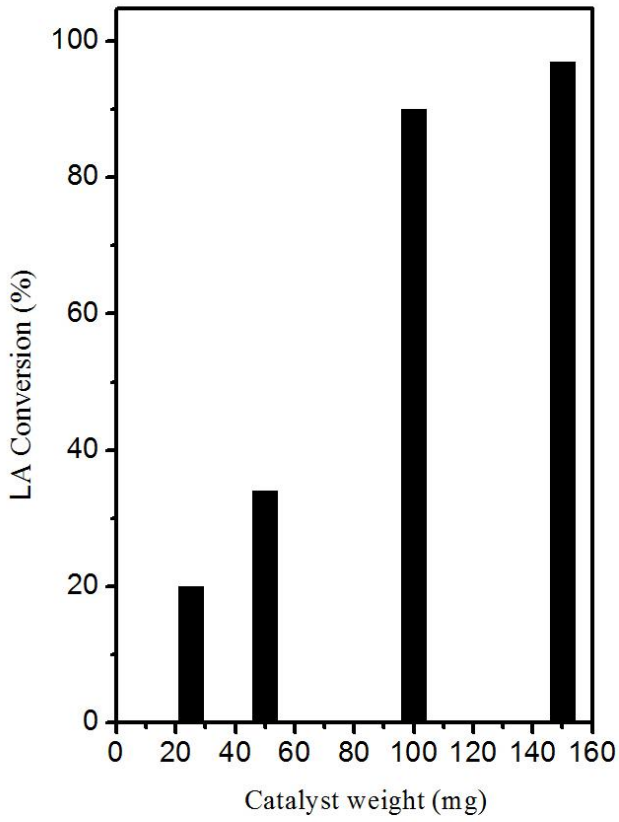

Fig.12.

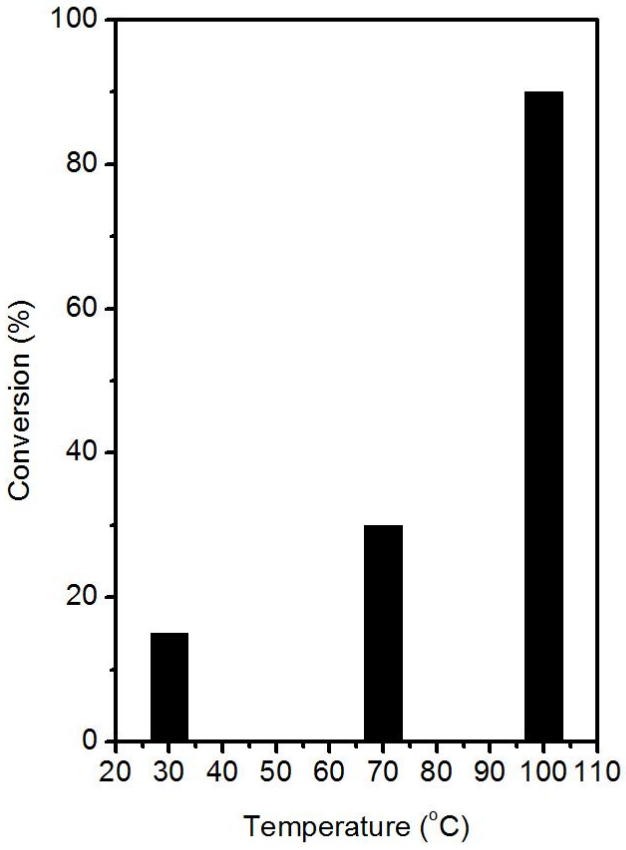

Fig.13.

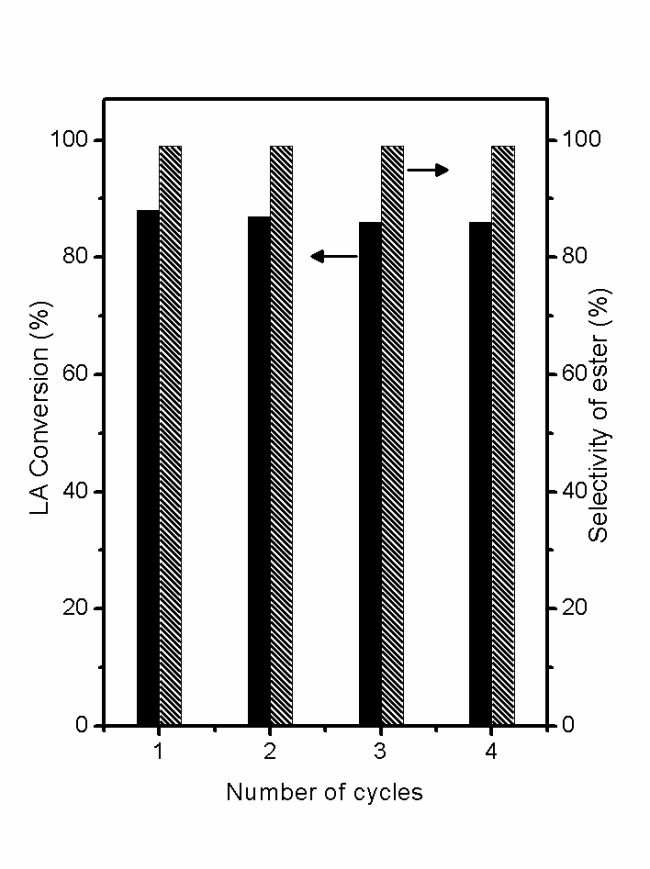

Fig.14.

Table 1. Textural characteristics of supports and catalysts obtained from N_2 adsorption

Catalyst	**Total surface area (m^2/g)**	**External surface area (m^2/g)**	**Micropore surface area (m^2/g)**	**Total pore volume (cm^3/g)**
C-Sil-1	358	76	282	0.178
HPA/C-Sil-1	237	128	109	0.120
Sil-1	253	25	228	0.152
HPA/Sil-1	190	95	95	0.119

Table 2. Catalytic activity of the catalysts in esterification of levulinic acid

Catalyst	**Conversion of LA with different alcohols (%)***		
	1-Propanol	**1-Butanol**	**1-Heptanol**
No catalyst	11	10	13
HPA/C-Sil-1	90 (99)	93 (99)	76 (92)
HPA/Sil-1	31 (99)	29 (98)	34 (90)
HPA**	38 (99)	35 (99)	36 (98)
C-Sil-1	15	13	16
Sil-1	13	11	15

*Reaction parameters: temperature = 100 ^{o}C, 1- propanol : LA mole ratio = 5:1, catalyst weight = 100 mg; reaction time = 5 h

**Catalyst weight = 35 mg

Values given in the parenthesis indicate selectivity of the corresponding ester product